Stem Cell Reports, Volume *4*

Supplemental Information

Kinome-wide shRNA Screen Identifies the Receptor Tyrosine Kinase *AXL* as a Key Regulator for Mesenchymal Glioblastoma Stem-like Cells

Peng Cheng, Emma Phillips, Sung-Hak Kim, David Taylor, Thomas Hielscher, Laura Puccio, Anita Hjelmeland, Peter Lichter, Ichiro Nakano, and Violaine Goidts

Figure S1

A

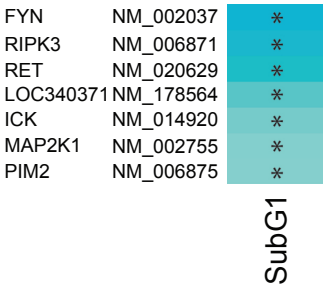
FYN NM_002037
RIPK3 NM_006871
RET NM_020629
LOC340371 NM_178564
ICK NM_014920
MAP2K1 NM_002755
PIM2 NM_006875
SubG1

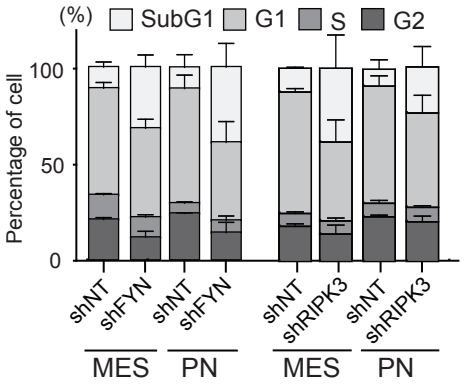
(%)
SubG1
G1
S
G2
Percentage of cell
100
50
0
shNT
shFYN
shNT
shFYN
shNT
shRIPK3
shNT
shRIPK3
MES
PN
MES
PN

B

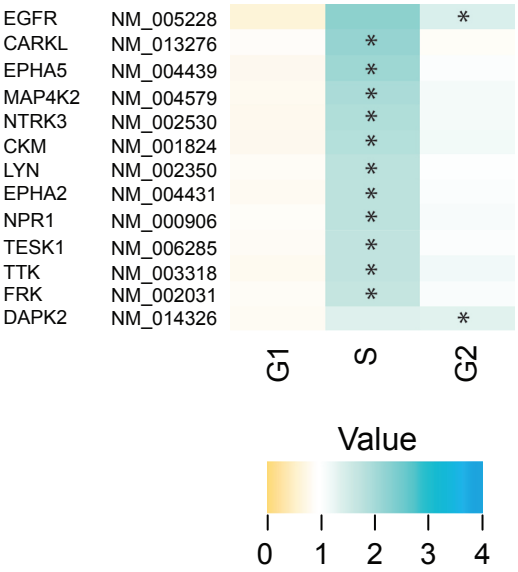
EGFR NM_005228
CARKL NM_013276
EPHA5 NM_004439
MAP4K2 NM_004579
NTRK3 NM_002530
CKM NM_001824
LYN NM_002350
EPHA2 NM_004431
NPR1 NM_000906
TESK1 NM_006285
TTK NM_003318
FRK NM_002031
DAPK2 NM_014326
G1
S
G2
Value
0
1
2
3
4

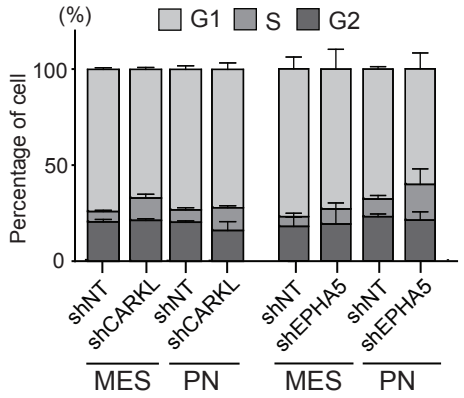
(%)
G1
S
G2
Percentage of cell
100
50
0
shNT
shCARKL
shNT
shCARKL
shNT
shEPHA5
shNT
shEPHA5
MES
PN
MES
PN

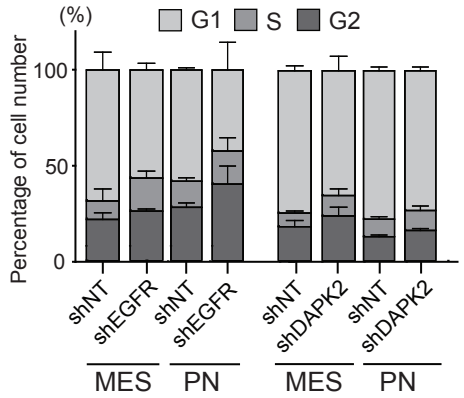
(%)
G1
S
G2
Percentage of cell number
100
50
0
shNT
shEGFR
shNT
shEGFR
shNT
shDAPK2
shNT
shDAPK2
MES
PN
MES
PN

Figure S2

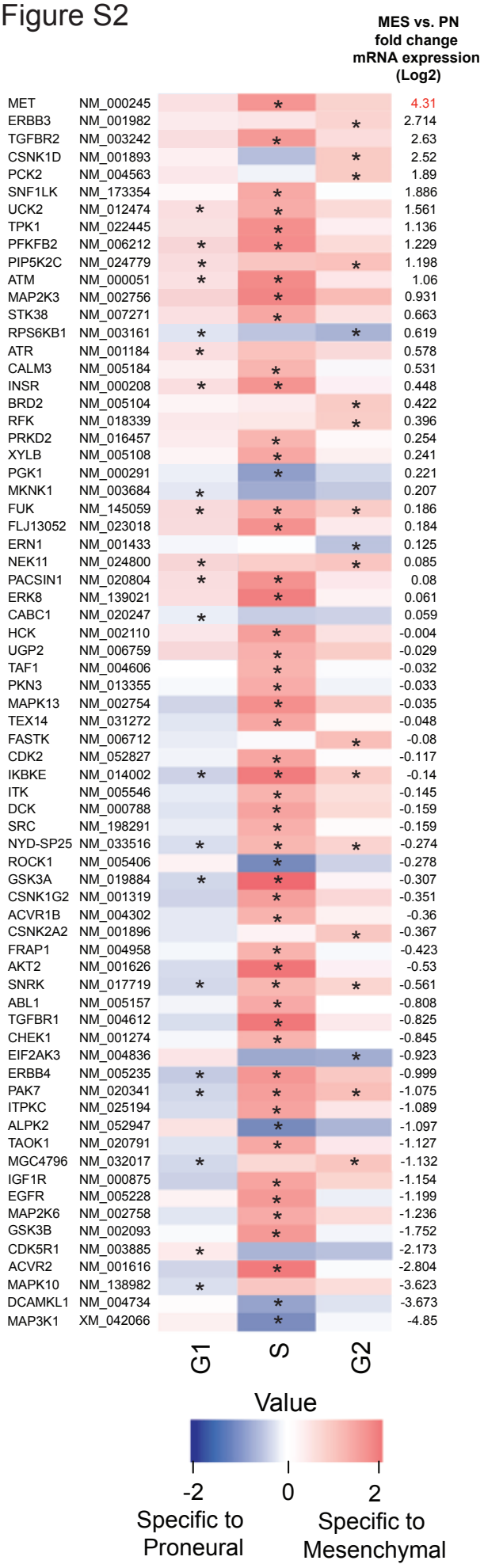
MES vs. PN
fold change
mRNA expression
(Log2)
MET NM_000245 4.31
ERBB3 NM_001982 2.714
TGFBR2 NM_003242 2.63
CSNK1D NM_001893 2.52
PCK2 NM_004563 1.89
SNF1LK NM_173354 1.886
UCK2 NM_012474 1.561
TPK1 NM_022445 1.136
PFKFB2 NM_006212 1.229
PIP5K2C NM_024779 1.198
ATM NM_000051 1.06
MAP2K3 NM_002756 0.931
STK38 NM_007271 0.663
RPS6KB1 NM_003161 0.619
ATR NM_001184 0.578
CALM3 NM_005184 0.531
INSR NM_000208 0.448
BRD2 NM_005104 0.422
RFK NM_018339 0.396
PRKD2 NM_016457 0.254
XYLB NM_005108 0.241
PGK1 NM_000291 0.221
MKNK1 NM_003684 0.207
FUK NM_145059 0.186
FLJ13052 NM_023018 0.184
ERN1 NM_001433 0.125
NEK11 NM_024800 0.085
PACSIN1 NM_020804 0.08
ERK8 NM_139021 0.061
CABC1 NM_020247 0.059
HCK NM_002110 -0.004
UGP2 NM_006759 -0.029
TAF1 NM_004606 -0.032
PKN3 NM_013355 -0.033
MAPK13 NM_002754 -0.035
TEX14 NM_031272 -0.048
FASTK NM_006712 -0.08
CDK2 NM_052827 -0.117
IKBKE NM_014002 -0.14
ITK NM_005546 -0.145
DCK NM_000788 -0.159
SRC NM_198291 -0.159
NYD-SP25 NM_033516 -0.274
ROCK1 NM_005406 -0.278
GSK3A NM_019884 -0.307
CSNK1G2 NM_001319 -0.351
ACVR1B NM_004302 -0.36
CSNK2A2 NM_001896 -0.367
FRAP1 NM_004958 -0.423
AKT2 NM_001626 -0.53
SNRK NM_017719 -0.561
ABL1 NM_005157 -0.808
TGFBR1 NM_004612 -0.825
CHEK1 NM_001274 -0.845
EIF2AK3 NM_004836 -0.923
ERBB4 NM_005235 -0.999
PAK7 NM_020341 -1.075
ITPKC NM_025194 -1.089
ALPK2 NM_052947 -1.097
TAOK1 NM_020791 -1.127
MGC4796 NM_032017 -1.132
IGF1R NM_000875 -1.154
EGFR NM_005228 -1.199
MAP2K6 NM_002758 -1.236
GSK3B NM_002093 -1.752
CDK5R1 NM_003885 -2.173
ACVR2 NM_001616 -2.804
MAPK10 NM_138982 -3.623
DCAMKL1 NM_004734 -3.673
MAP3K1 XM_042066 -4.85
G1
S
G2
Value
-2
0
2
Specific to Proneural
Specific to Mesenchymal

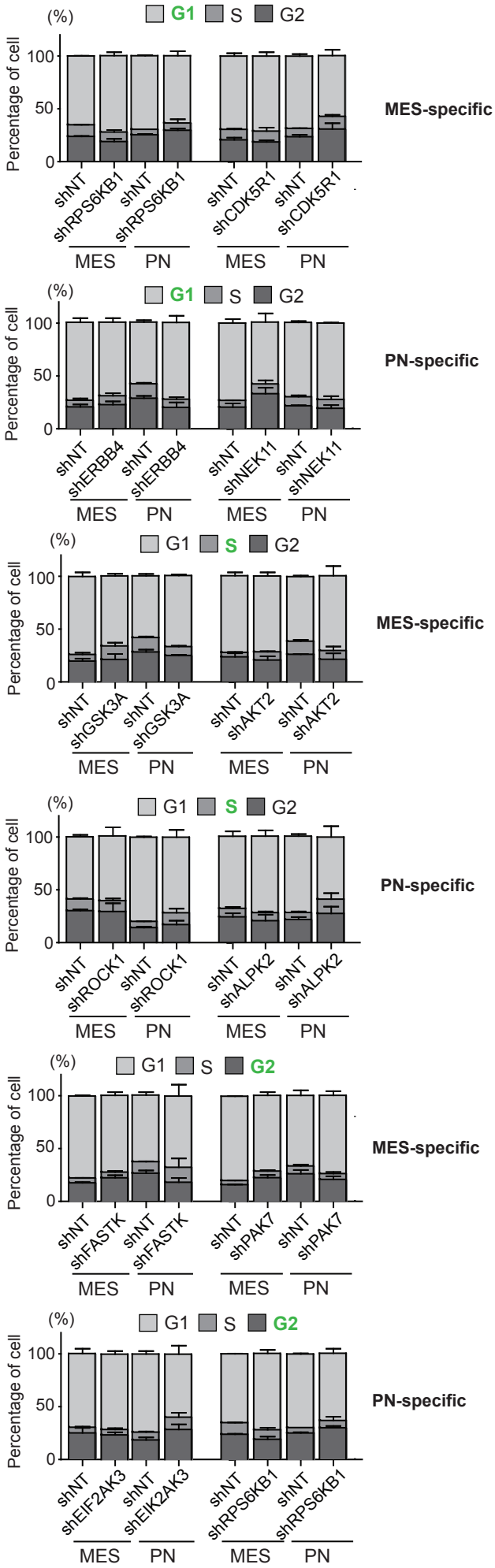
(%)
G1
S
G2
Percentage of cell
100
50
0
shNT
shRPS6KB1
shCDK5R1
shERBB4
shNEK11
shGSK3A
shAKT2
shROCK1
shALPK2
shFASTK
shPAK7
shEIF2AK3
MES
PN
MES-specific
PN-specific
MES-specific
PN-specific
MES-specific
PN-specific

Figure S3

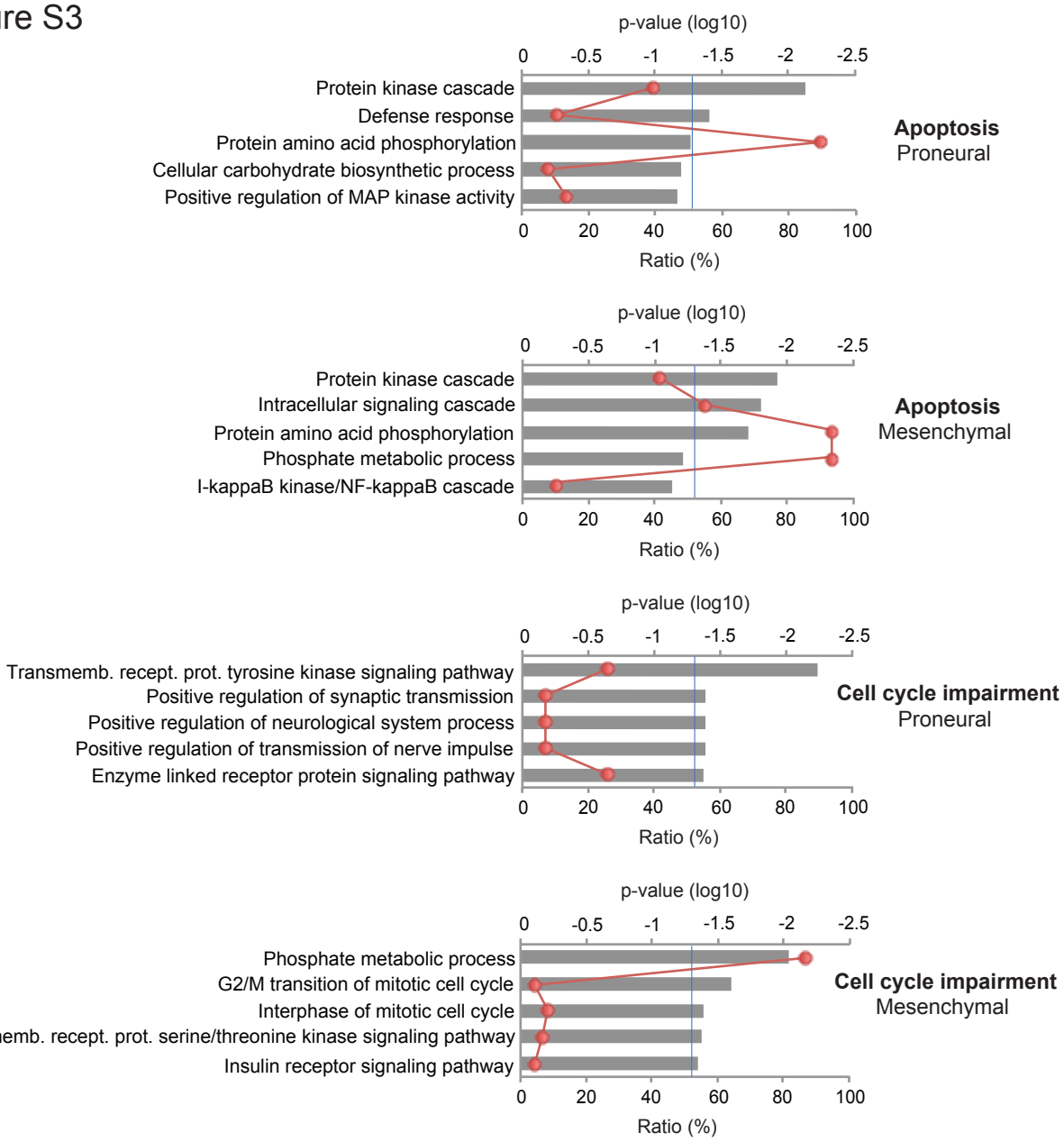
p-value (log10)
0 -0.5 -1 -1.5 -2 -2.5
Protein kinase cascade
Defense response
Protein amino acid phosphorylation
Cellular carbohydrate biosynthetic process
Positive regulation of MAP kinase activity
0 20 40 60 80 100
Ratio (%)
Apoptosis
Proneural
p-value (log10)
0 -0.5 -1 -1.5 -2 -2.5
Protein kinase cascade
Intracellular signaling cascade
Protein amino acid phosphorylation
Phosphate metabolic process
I-kappaB kinase/NF-kappaB cascade
0 20 40 60 80 100
Ratio (%)
Apoptosis
Mesenchymal
p-value (log10)
0 -0.5 -1 -1.5 -2 -2.5
Transmemb. recept. prot. tyrosine kinase signaling pathway
Positive regulation of synaptic transmission
Positive regulation of neurological system process
Positive regulation of transmission of nerve impulse
Enzyme linked receptor protein signaling pathway
0 20 40 60 80 100
Ratio (%)
Cell cycle impairment
Proneural
p-value (log10)
0 -0.5 -1 -1.5 -2 -2.5
Phosphate metabolic process
G2/M transition of mitotic cell cycle
Interphase of mitotic cell cycle
Transmemb. recept. prot. serine/threonine kinase signaling pathway
Insulin receptor signaling pathway
0 20 40 60 80 100
Ratio (%)
Cell cycle impairment
Mesenchymal

Figure S4

MES_83
shAXL#2

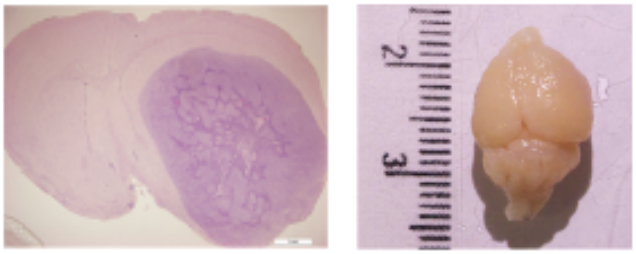

30 days

Figure S5

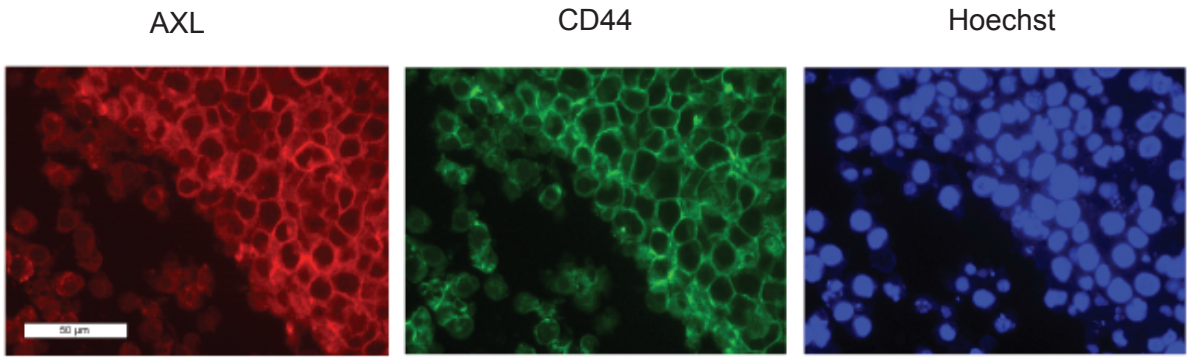

Supplementary Figure legends

Figure S1: Knockdown of a subset of kinases decreases viability and alters cell cycle of both MES and PN GSCs. Related to Figure 1

(A) Kinases that induce a significant level of cell death (*: $p<0.05$) in MES and PN GSCs when targeted with shRNA. The color code represents the fold increase of SubG1 phase cells after knockdown of the indicated gene compared to cells transduced with a non-targeting shRNA (shNT).

(B) Kinases that significantly alter the cell cycle in MES and PN GSCs (*. $p<0.05$) when targeted with shRNA. The color code represents the fold increase of cell numbers in the respective cell cycle phases compared to cells transduced with shNT. Stacked bar charts on the right panels represent the percentage of cells in the different phases of the cell cycle in MES and PN GSCs for the top two genes in each of the indicated cell cycle phases, as determined by FACS analysis of propidium iodide DNA staining. The average of the shNT used for normalization and the shRNAs targeting the indicated gene are shown. Error bars represent the standard deviation.

Figure S2: Knockdown of a subset of kinases differentially alters cell cycle in MES or PN GSCs. Related to Figure 2

(A) List of kinases that significantly (*: $p<0.05$) impair the cell cycle in MES GSCs (blue) or in PN GSCs (red) when targeted with shRNA. Data were normalized to the respective shNT. mRNA expression fold change between PN and MES GSCs is

indicated on the right side of the heatmap.

(B) Stacked bar charts depicting cell percentage of the top two genes in each cell cycle phase that when targeted with shRNA significantly impair the cell cycle. Average of the shNT used for normalization and the shRNAs targeting the indicated gene are shown. Error bars represent the standard deviation.

Figure S3: Gene ontology analysis using the DAVID tool of the candidate genes that impair MES or PN viability. Related to Figure 2

Kinases whose silencing increases SubG1 phases (described as apoptosis kinases) were separated from those that impair G1, S or G2 phases (described as proliferation impairing kinases). The human kinome was used as background to ensure statistical correctness.

Figure S4: Representative photographs of mice brains. Related to Figure 5

Animals were injected with 83 GSCs transduced with shAXL#2 and representative H&E staining of shAXL mouse xenografts, 30 days after transplantation, is shown.

Figure S5: Staining of AXL and CD44. Related to Figure 6

Staining was perfomed on a mouse brain tumor sample close to a necrotic area (83 GSCs). Scale bar: 50 μm.

Materials and methods

Lentiviral Production and Transduction

To assess transduction efficiency, cells on each plate were infected with lentivirus expressing green fluorescent protein (GFP). Transduction was deemed efficient if >70% cells were GFP-expressing. To reduce any position effects, the 3-5 shRNAs targeting each kinase where divided onto two plates and each plate included three replicates of a non-targeting shRNA (shNT). Measurements were standardized by the average of the shNT measurements separately for each plate. The titer was measured using lentiviral particles that contained the pLKO.1 vector expressing GFP and ranged from 2×10^6 to 4×10^6 Transduction Units/ml. Transductions were performed at the multiplicity of infection (MOI) of 10.

Reagents and Antibodies

The following primary antibodies and reagents were used in this study: EGF (Peprotech); bFGF (Peprotech); B27 (invitrogen); Heprin (Sigma); DMEM-F12 (Gibco, 10565-018); anti-AXL (Cell signaling, #8661) for immunocytochemistry, immunoflurescence and Western blot, anti-phospho-AXL (R&D AF2228) for immunocytochemistry, immunohistochemistry and Western blot; anti-GAPDH (Abcam, ab9482) for Western blot; anti-CD44 (Cell Signaling #3570) for immunofluorescence and (Miltenyl Biotec #130-090-854) for FACS; and anti-CD133 (Biolegend #103016) for FACS. Fetal bovine serum (Gibco, 10082-147); Albumin from bovine serum (Sigma, A2153); Accutase solution (Sigma, A6964-100); alamar

Blue (invitrogen, DAL1100); RIPA buffer (Sigma, R0278-50ml); Phophatase inhibitor cocktail (Sigma, P0044-5ml); Protease inhibitor cocktail (P8340); Bradford (BIO-RAD, 500-0006); BSA used in Bradford assay (BioLabs, B9001S); PageRuler plus prestained protein (Thermo scientific, 26619);. iScript Reverse Transcription supermix for RT-qPCR (Bio-rad, 170-8841); Caspase-Glo®3/7 Assay (Promega).

Western blot analysis

The cell lysates were prepared in RIPA buffer containing protease and phosphatase inhibitor cocktail (Sigma Aldrich) on ice. The sample protein concentrations were determined by the Bradford method. Equal amounts of protein lysates (10 μg/lane) were fractionated on NuPAGE Novex 4-12% Bis-Tris Protein gel (Invitrogen) and transferred to a PVDF membrane (Invitrogen). Subsequently, the membranes were blocked with 5% skimmed milk for 1 h and then treated with the relevant antibody at 4°C overnight. Protein expression was visualized with Amersham ECL Western Blot System (GE Healthcare Life Sciences). GAPDH served as a loading control.

Quantitative RT-PCR

Total RNA was prepared using a RNeasy mini kit (Qiagen) according to the manufacturer's instructions. RNA concentration was determined using a Nanodrop 2000 (Thermo scientific). RNA integrity was examined with an Agilent 2100 Bioanalyzer. For reverse transcription, the average RNA integrity number (RIN) was larger than 9.0. cDNA was synthesized by using iScript reverse transcription

supermix for RT-qPCR (Bio-rad) according to the manufacturer's protocol. Quantitative RT-PCR was performed using a StepOnePlus real-time PCR system with a SYBR Select Master Mix (Applied Biosystems). GAPDH was used as an internal control. The following cycles were performed during DNA amplification: 94°C for 2 min, 50 cycles of 94°C (30 s), 60°C (30 s), and 72°C (40 s). The primer sequences for qPCR were as follows:

AXL forward: GTTTGGAGCTGTGATGGAAGGC;

AXL Reverse: CGCTTCACTCAGGAAATCCTCC (Gioia et al., 2011);

CD44 forward: CCCAGATGGAGAAAGCTCTG;

CD44 reverse: ACTTGGCTTTCTGTCCTCCA;

CD133 Forward: ACTCCCATAAAGCTGGACCCC;

CD133 Reverse: TCAATTTTGGATTCATATGCCTT;

GAPDH forward: GAAGGTGAAGGTCGGAGTCA;

GAPDH reverse: TTGAGGTCAATGAAGGGGTC.

Relative quantitation of cDNAs to *GAPDH* was determined by $2^{-\Delta\Delta Ct}$ method.

Statistical analysis

For analysis of FACS data, measurements with less than 2000 cell counts were excluded. Measurements were standardized by the average of the non-target shRNA measurements separately for each plate. Ratios were log2 transformed to more closely follow a normal distribution. Relevant kinase directed shRNAs were identified using the empirical Bayes approach (Smyth, 2004) based on moderated t-statistics

as implemented in the Bioconductor package limma (Smyth, 2005). Kinase directed shRNAs with differential activity between cell lines were identified for each cycle phase separately using one-sided p-values and a fold change (FC) threshold of the median FC plus two median absolute deviations. shRNAs showing an equivalent increase of cell number in the respective cell cycle phase in both cell lines were defined based on the following criteria: increase across cell lines was determined as for individual cell lines but based on shRNAs from both cell lines pooled using one-sided p-values and a FC threshold. The two-sided 90 % confidence interval for the difference between both cell lines was computed. Confidence limits had to fall within pre-specified boundaries in order to establish equivalence. Boundaries were defined in terms of acceptable absolute FC. Since magnitude and variability of cell number levels were very different for each cycle phase, different equivalence boundaries (FC 1.1 to 1.6) were applied for each phase. All p-values were adjusted for multiple testing using Benjamini-Hochberg correction in order to control the false discovery rate. Adjusted p-values below 0.05 were considered statistically significant. All analyses were carried out using software R 3.0.1. (Team, 2011).

MACS Cell Separation

PN_528 GSCs were separated according to their level of CD133 expression by MACS according to manufacturer's instruction. In brief, single cell suspensions were prepared with Accutase (Life technology). After 30 mins incubation with CD133 MicroBeads (Miltenyi Biotec) at 4°C, cells were added on LS columns (Miltenyi

Biotec) and placed in a MidiMACS separator. The flow-though cells were collected as CD133 low cells. The cell fraction retained in the column was eluted as CD133 high cells.

REFERENCES

Gioia, R., Leroy, C., Drullion, C., Lagarde, V., Etienne, G., Dulucq, S., Lippert, E., Roche, S., Mahon, F.X., and Pasquet, J.M. (2011). Quantitative phosphoproteomics revealed interplay between Syk and Lyn in the resistance to nilotinib in chronic myeloid leukemia cells. Blood *118*, 2211-2221.

Smyth, G.K. (2004). Linear models and empirical bayes methods for assessing differential expression in microarray experiments. Statistical applications in genetics and molecular biology *3*, Article3.

Smyth, G.K. (2005). Limma: linear models for microarray data (New York: Springer).

Team, R.D.C. (2011). R: A language and environment for statistical computing. (Vienna, Austria: R Foundation for Statistical Computing).